22.0 DEVELOPMENT OF NOVEL HIGH TEMPERATURE ALUMINUM ALLOYS

Joe Jankowski (CSM)
Faculty: Michael Kaufman (CSM), Amy Clarke (CSM), Robert Field (CSM), and Steve Midson (CSM)
Industrial Mentor: Krish Krishnamurthy (Honeywell) and Paul Wilson (Boeing)

This project initiated in Summer 2015 and is supported by CANFSA. The research performed during this project will serve as the basis for a Ph.D. thesis for Joe Jankowski.

22.1 Project Overview and Industrial Relevance

The purpose of this project is to develop a high-performance structural aluminum alloy with acceptable high temperature strength through the formation of a lamellar microeutectic microstructure composed of aluminum and the cubic intermetallic phase α-$Al_{13}(Fe,V)_3Si$, similar to the dispersoid strengthening used in RS8009. The reason this alloy is of particular interest is that this microstructure can be formed at cooling rates of 10^2 to 10^3 K/s, orders of magnitude lower than rapid solidification (RS) cooling rates. This suggests this alloy system could represent a lower cost alternative to current high-temperature aluminum alloys produced by rapid solidification (e.g., RS8009), or by related methods such as powder metallurgy. The development of a lower cost aluminum alloy with acceptable high temperature mechanical properties would allow for improvements in part performance in industries where current RS alloys are prohibitively expensive.

In order to develop an alloy system that has acceptable high temperature mechanical properties, it is critical to minimize or prevent the formation of unwanted phases while producing a significant volume fraction and distribution of a desirable strengthening phase(s). In the case of the AlFeVSi system, the hexagonal $Al_{12.8}(Fe,V)_3Si_{0.3}$ phase (h-phase) needs to be avoided because it forms with a coarse, dendritic morphology rather than as a fine dispersoid. The h-phase has a composition and crystal structure that are similar to those of the $Al_{13}(Fe,V)_3Si$ α-phase. Additionally, due to the high content of Fe in the baseline 8009 alloy, large $Al_{13}Fe_4$ (θ-phase) particles may form in 1 cm diameter chill castings. It is therefore essential that alloying strategies promote fine α-phase, while suppressing the coarser, detrimental h-phase and θ-phase. To this end, concepts from physics/chemistry are used to identify the workable composition space and are supplemented by density functional theory (DFT) calculations and data from the literature.

The detailed characterization of the h-phase and incorporation of electronic structure information can not only be used to promote the microeutectic constituent containing α-$Al_{13}(Fe,V)_3Si$ and aluminum, but may also provide information about how to improve existing RS alloys and develop new alloys optimized for additive manufacturing. Commercial RS8009 alloys are known to contain a small amount of the h-phase, which is coarser than the desired dispersion of α-$Al_{13}(Fe,V)_3Si$ [22.1]. The use of conceptual tools from chemistry and physics, coupled with DFT, should allow for the rapid optimization of microeutectic volume fraction in a large composition space. The methodology used in this work will be applicable to essentially all Al-TM (transition metal) and Al-TM-Si alloys.

22.2 Previous Work

Several important findings were made prior to this reporting period. First, the as-cast microeutectic structure in 8009 chill castings was found to have hardness values comparable to extruded RS8009, and was microstructurally stable at temperatures well above target operating temperatures (250 to 300 °C). The thermal stability and high hardness of the microeutectic constituent were two of the initial findings that suggested its potential for high temperature applications. Since high hardness alone is not sufficiently indicative of desirable mechanical properties, a three-point bending test was performed on a sample that contained a significant volume fraction of the microeutectic constituent. The fracture surface displayed ductile fracture features. The high hardness, thermal stability, and ductility of the microeutectic constituent indicated that, if it can be produced throughout a cast part, desirable mechanical properties would likely result.

Another important result was the development of a detailed crystal structure model for the h-phase using synchrotron x-ray and neutron powder diffraction at U.S. DOE user facilities, coupled with charge flipping [22.2] for determining the crystal structure. Based on this model, minor alloying additions of Co and Mn and major alloying additions of Si were examined and found to be beneficial for suppressing the h-phase, where the Si additions were especially effective. DFT calculations on the $Pm\bar{3}$ AlMnSi-type structure for the α-phase [22.3] were used to determine workable compositions for the α-phase in Al alloys. It was found that V, Cr, Mo, Mn, and Fe were effective in stabilizing the

α-phase and compositional rules for incorporating them were developed. Experimentally, small additions of B were found to promote α-phase particle nucleation in Al-Fe-Mn-Cr-Si alloys.

The crystallography of the α-phase was examined as a function of composition and processing conditions in Al-Fe-Cr-Si and Al-Fe-V-Si alloys with minor B additions for inoculation (B only effectively inoculates the α-phase in Al-Fe-Cr-Si). Characterization was performed using electron microprobe analysis (EPMA) and synchrotron x-ray powder diffraction. It was found that, in the as-cast condition for both Cr and V containing alloys, the composition and crystallography of the α-phase could be substantially different from the heat-treated condition and from what is reported in the literature [22.4]. Additionally, in the Al-Fe-V-Si alloys, the h-phase was present, despite the high Si content, and the as-cast α-phase possessed an undesirable morphology and potentially undesirable stoichiometry. Based on the potentially unfavorable results in the Al-Fe-V-Si alloys, the Al-Fe-Cr-Si alloy system was chosen as a baseline going forward. In practice, the Al-Fe-Mn-Cr-Si alloy system was examined due to its improved processibility.

Process control during casting was refined by developing a new casting protocol to improve consistency. Cooling rates were measured using secondary dendrite arm spacing in the reference alloy A356 [22.5], since cooling rate is a quantitative indicator of the solidification conditions in the casting. Cooling rates can also be used as part of future in-depth solidification studies.

22.1 Recent Progress

22.1.1 Processing-Microstructure Study and Subsequent Optimization

The initial goal of the processing-microstructure study was to build an experimental matrix of compositions and processing conditions for Al-Fe-Mn-Cr-Si alloys to determine how high volume fractions of the Al-α microeutectic constituent could be produced in chill castings. The compositions examined in this study are shown in **Table 22.1**. The compositions are based on Thermo-Calc determinations of equilibrium liquidus temperatures and the stoichiometry of the as-cast α-phase determined from previous EPMA characterization [22.4]. Processing conditions were varied by casting into a stepped cylindrical Cu chill mold, as illustrated in **Figure 22.1**, at different melt superheats for each composition. This experimental matrix produced a range of compositions, melt superheats, and cooling rates in the castings. The melt superheats examined were 50 °C and 200 °C. Additionally, each cylinder possessed different solidification velocities and thermal gradients, although these characteristics were not quantified.

In order to analyze the large number of samples generated in this study, the scope of characterization was limited to optical microscopy (OM) for most samples. Using OM, the probability of finding a particular microstructural constituent was determined as a function of distance from the mold wall in the plane halfway between the top and bottom of each diameter of cylinder for each melt superheat and composition examined. Lengths along the centerline were binned, and the presence of any detectable amount of a constituent in a given bin was included in a calculation of the probability of observing a given constituent as a function of distance from the mold wall. The calculated probability is related to the likelihood of observing a given constituent, but is not related to the volume fraction of that constituent. A probability of 100% means a given constituent was observed in all bins, but with potentially varying volume fractions. Two of the most important results of this study, which are discussed further below, are shown in **Figure 22.2** to illustrate the plots generated from this analysis. The microstructural constituents identified for this analysis were “primary Al,” “eutectic islands,” and “primary α.” Pictures for each constituent are shown in **Figure 22.3**.

The probability of primary α decreased as melt superheat increased in the J40 alloy in the 4mm diameter section of the casting. This seemingly contradictory trend can be rationalized, though, considering that J40 is a hypereutectic composition. High undercoolings in hypereutectic alloys can lead to fine primary dispersoids of the secondary phase, like in 8009. Higher superheats would be expected to reduce the undercoolings achieved and suppress primary α formation. The other constituent present in these castings was primary Al. The presence of primary Al suggests that the undercoolings being achieved are below the coupled growth region; lower cooling rates would promote a high volume fraction of microeutectic. This is schematically illustrated in **Figure 22.4**. In order to lower cooling rates without altering mold geometry, a BN coating was applied to the mold [22.6] and a melt superheat of 200 °C was used. This process successfully produced castings with relatively high volume fractions of microeutectic, although high volumes of primary Al were also observed. Once a process was developed for producing relatively high volume fractions of microeutectic, Vickers microhardness and compression tests were performed.

22.1.2 Mechanical Testing of J40 and J35 Alloys

The microhardness testing results for J35 and J40 are shown in **Table 22.2**. The yield strength for all three J40 samples tested in compression (all were 4mm in diameter, taken from different castings) was approximately 30 ksi with a substantial work hardening response. Interestingly, when the deformed microstructure was examined with microhardness testing, it was found that the primary Al region, which contains a solute-rich microeutectic constituent, was stronger in both the as-cast and deformed conditions and appeared to experience a substantial work hardening response, unlike the fully microeutectic region. The higher hardness of the primary Al microstructure, with its interdendritic solute-rich microeutectic, suggests it may be preferable to the fully microeutectic microstructure. This appears to be due to a transition from a rod-like to lamellar microeutectic at higher transition metal contents.

Fortunately, as shown in **Figure 22.2b**, a processing condition and composition had already been identified that were optimal for producing a fully primary Al microstructure. The J35 alloy cast with a superheat of 200 °C exhibited a reproducible microstructure of through-thickness primary Al for diameters of 4 and 6 mm. Further mechanical testing was performed on the 6 mm section, due to the lower cooling rates required to develop the desired microstructure, consistent with the initial goal of making an Al alloy producible at relatively low cooling rates (100-1,000 K/s). A summary of the room temperature and elevated temperature compression data is shown in **Table 22.3**. Although full characterization of the microstructures has not been performed, the elevated temperature mechanical properties are impressive. **Figure 22.5** shows the yield strength of J35 compared to 2219, NASA 398, and RS8009 as a function of testing temperature. 2219 is a wrought alloy for elevated temperature applications, NASA 398 has the highest elevated temperature strength of conventionally processed Al to the authors' knowledge, and RS8009 is an Al "superalloy" produced by rapid solidification and powder metallurgy. It can be seen that the performance of J35 exceeds 2618 and NASA 398 at very high temperatures, due to superior microstructural stability, and is around half the strength of RS8009 throughout the temperature range examined. Interestingly, the strength of J35 increases after a 100 hr hold at 260 °C. In that condition the strength is around 70 percent of the strength of RS8009, surpassing all conventionally processed alloys the authors are aware of.

Further characterization of J35 held at 260 °C for 100 h is underway in order to better understand the unexpected increase in yield strength.

22.1.3 Autogenous Gas Tungsten Arc Welding (GTAW) Solidification Study

Although the chill mold was useful to manufacture samples for mechanical testing and microstructural characterization in the processing-microstructure study, it provides little insight into important solidification characteristics such as thermal gradients and solidification velocities. To address this issue, autogenous GTAW welds will be made on J35 plates to examine their solidification microstructures with known solidification velocities. The cooling rates can also be approximated. In combination with known solidification velocity, thermal gradients can be estimated. To this end, a new Cu chill mold has been manufactured to make castings with the approximate dimensions 4 x 40 x 40 mm. The cast plates are rolled to an approximate final dimension of 2 x 40 x 80 mm prior to performing the weld. A demonstration weld has already been made using GTAW with 110 A alternating current (AC) at a travel speed of approximately 4 mm/s to demonstrate the viability of this process. The melt pool appeared to fully melt in the center, although some particles along the edge of the melt pool suggest regions of only partial metling.

22.2 Plans for Next Reporting Period

The processing-microstructure study enabled successful production of mechanical testing specimens tested in compression to evaluate yield strength as a function of temperature for different morphologies of Al-α microeutectic-containing microstructures. The following tasks are planned for the next reporting period:

- Further investigate mechanical behavior of J35 after 100 h at 260 °C.
- Characterize the microstructure of as-cast and heat treated J35 using SEM, microprobe, and TEM.
- Characterize autogenous GTAW weld microstructures of J35 for different weld speeds and compare the results to data obtained in the processing-microstructure study.
- Confirm the validity of prior density functional theory (DFT) calculations on the α-phase.
- Write journal articles documenting the results of the project.

- Write Dissertation.

22.3 References

[22.1] R. Marshall. Characterization of Novel Microstructures in Al-Fe-V-Si and Al-Fe-V-Si-Y Alloys Processed at Intermediate Cooling Rates, Master's Thesis. Colorado School of Mines (2015).

[22.2] C. Baerlocher, L. B. McCusker, L. Palatinus. "Charge flipping combined with histogram matching to solve complex crystal structures from powder diffraction data," Z. Kristallogr. 222 (2007) 47–53.

[22.3] M. Cooper. "The crystal structure of the ternary alloy α(AlMnSi)," Acta Crystallographica. 20 (1966) 614-617.

[22.4] J. Jankowski *et al*. "Determination of the Intermetallic α-Phase Crystal Structure in Aluminum Alloys Solidified at Rapid Cooling Rates," In: C. Chesonis, (Ed.) Light Metals 2019. The Minerals, Metals, & Materials Society, 2019, pp. 121-127

[22.5] Q.G. Wang, D. Apelian, and D.A. Lados. "Fatigue behavior of A356/357 aluminum cast alloys. Part 1—Effect of casting defects," J. Light Metals **1** (2001) 85-97.

[22.6] H. S. Kim, I. S. Cho, J. S. Shin, S. M. Lee, and B. M. Moon. "Solidification Parameters Dependent on Interfacial Heat Transfer Coefficient between Aluminum Casting and Copper Mold," ISIJ International 45 (2005) 192-198.

22.4 Figures and Tables

Table 22.1: Alloy Compositions for Processing-Microstructure Study (at%)

Alloy	Al	Fe	Mn	Cr	Si
J35	Bal.	1.5	1.5	0.4	1.6
J40	Bal.	1.8	1.8	0.5	1.8
J45	Bal.	2.0	2.0	0.6	2.1
J50	Bal.	2.2	2.2	0.7	2.3

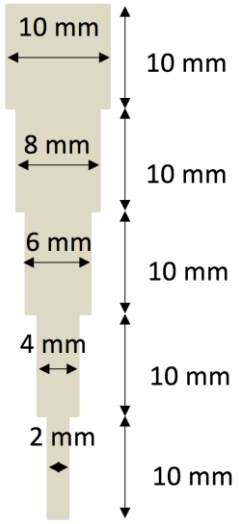

Figure 22.1: Illustration of the geometry of the Cu chill mold used for the processing-microstructure study.

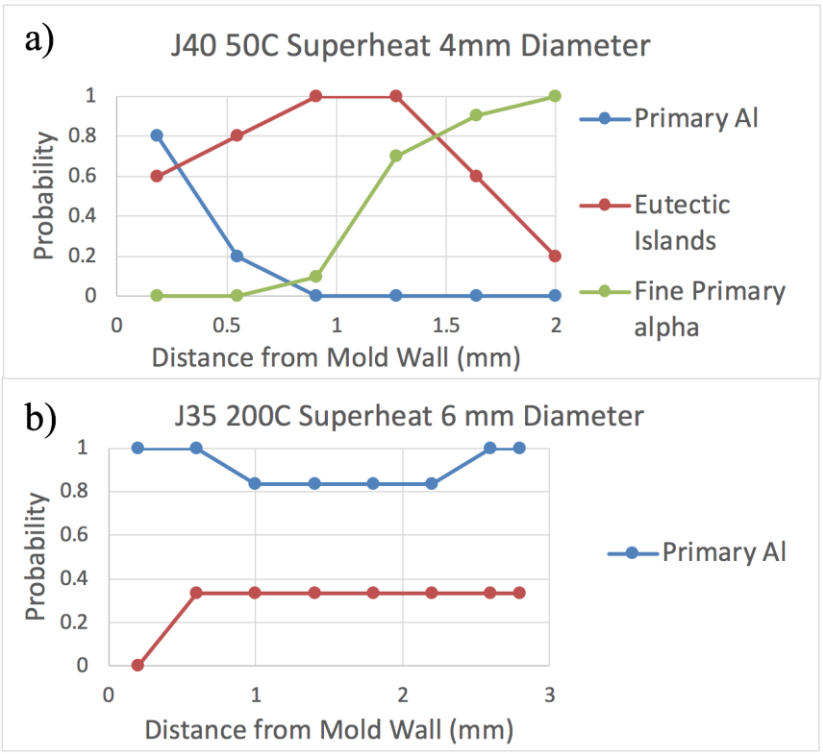

Figure 22.2: Probability-distance plots for the two processing conditions of highest interest. Probability indicates the likelihood of finding a given microstructural constituent at a given distance from the mold wall.

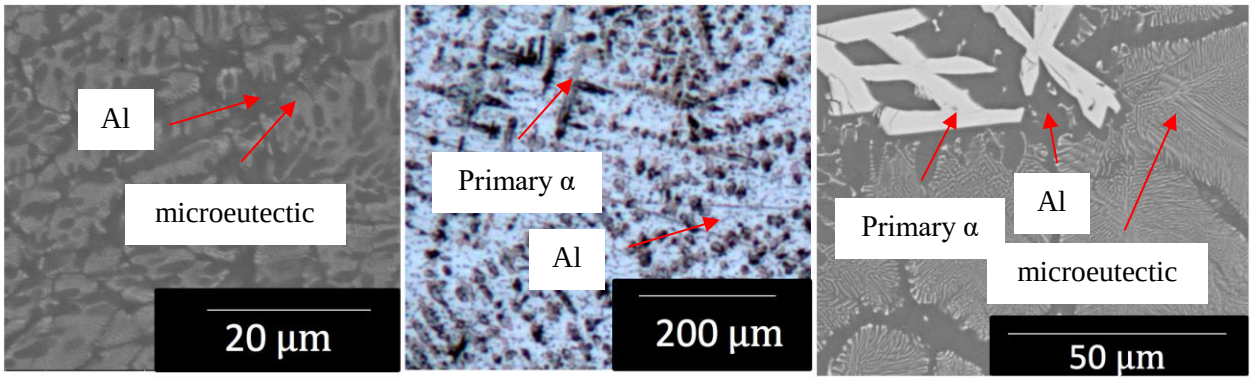

Figure 22.3: Example microstructures in J35 castings produced with a 200 °C superheat from left to right: "Primary Al" consisting of Al dendrites with interdendritic microeutectic (SEM), "Primary α" consisting of primary α particles with secondary Al and interdendritic phases which are the last to solidify (OM), and "Eutectic Islands" which consist of a primary α particle with an Al "halo" and eutectic Al-α colonies growing off of it (SEM).

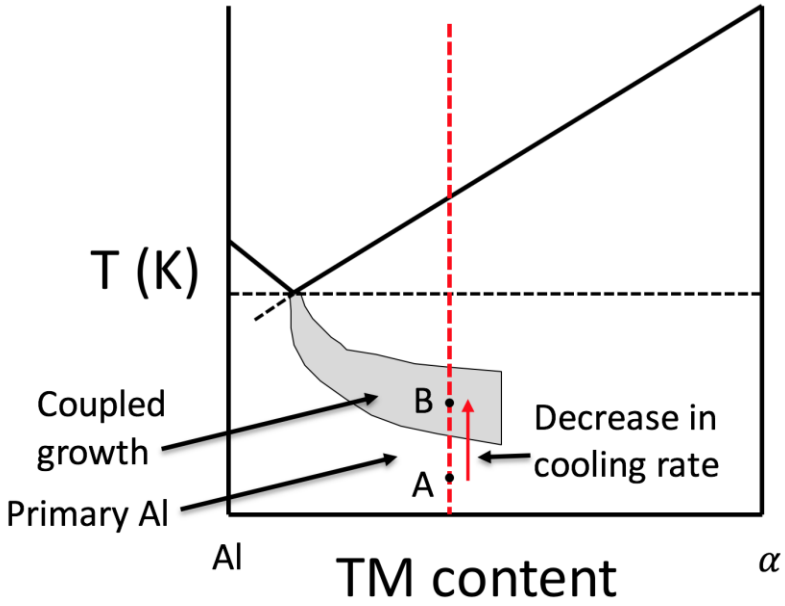

Figure 22.4: Schematic of requirements for coupled growth during solidification. Point A represents a condition under which primary Al would be expected to form and point B represents a condition under which fully coupled growth would form. Lower cooling rates would be expected to result in lower undercoolings and would therefore be expected to cause a primary Al growth condition to switch to a coupled growth condition. The axes shown are temperature and transition metal (TM) content of the melt.

Table 22.2: Microhardness (HV) results for J35 and J40 castings.

Alloy	**Diameter**	**Microstructure**	**Average Hardness (as-cast)**	**Average Hardness (deformed)**
J40	4 mm	Primary Al	104	140
J40	4 mm	Eutectic Islands	97	102
J35	6 mm	Primary Al	91	n/a
J35	6 mm	Eutectic Islands	80	n/a
J35	4 mm	Primary Al	100	n/a

Table 22.3: Summary of mechanical properties from compression testing on J35 6 mm diameter castings.

Hold Time at Temperature (hr)	**Testing Temperature (°C)**	**Yield Strength (ksi)**
n/a	25	32
0.5	260	20*
100	260	27
0.5	315	17
100	315	17*

0.5	370	14
100	370	14

*substantial scatter in results, highest value from 3 tests (each from a different casting) used

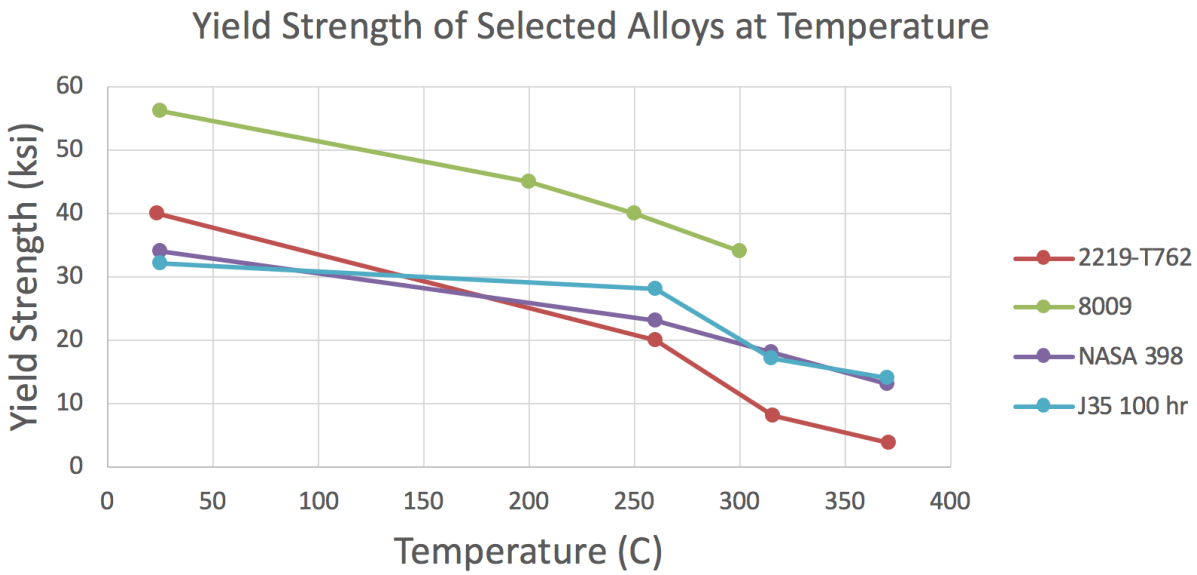

Figure 22.5: Yield strength of selected alloys as a function of test temperature. Samples were held for at least 100 hr at the test temperature prior to deformation. The hold time of J35 at temperature is 100 hr. The hold time of the other alloys varies but is equal to or greater than 100 hr. Yield strength values for J35 are estimated from 3 tests per condition. J35 appears to exhibit noticeable degradation of mechanical properties above 260 °C but this is a result of the anomalous yield strength at 260 °C.